

## Seismic Site Response Analysis of a Cairo Metro Tunnel

M. A. Adam<sup>1</sup>; A. M. Elleboudy<sup>2</sup>; and M. F. Soliman<sup>3</sup>

<sup>1</sup>Dept. of Civil Engineering, Faculty of Engineering-Shobra, Benha Univ., Cairo, Egypt. E-mail: [maher.adam@feng.bu.edu.eg](mailto:maher.adam@feng.bu.edu.eg)

<sup>2</sup>Dept. of Civil Engineering, Faculty of Engineering-Shobra, Benha Univ., Cairo, Egypt. E-mail: [prof.azza@feng.bu.edu.eg](mailto:prof.azza@feng.bu.edu.eg)

<sup>3</sup>Dept. of Civil Engineering, Faculty of Engineering-Shobra, Benha Univ., Cairo, Egypt. E-mail: [mustafa.soliman@feng.bu.edu.eg](mailto:mustafa.soliman@feng.bu.edu.eg)

### Abstract

Cairo metro network is one of the major national projects in Egypt. It aimed at developing underground transportation system to solve the severe traffic problems in Greater Cairo which includes 3 crowded governorates; Cairo, Giza and Qalyubia. The project started in the last decades of the twentieth century where 2 lines were executed. In this century, the project is expanding and more lines are constructed. The tunnel constructed for Cairo Metro Line 3 has a circular cross section that consists of a precast segmental lining thickness of 0.40 m. This paper presents a parametric study on the effects of seismic waves on the tunnel structure through numerous simulations employing the finite – element analysis. Full dynamic analyses were performed employing three different earthquake motions as well as the effect of train-induced dynamic load. Also, the induced tunnel straining actions were studied. The analysis of soil-structure interaction was done using the commercial software PLAXIS<sup>®</sup>. The results proved that the 0.40 m thick circular cross section can safely sustain the expected static, dynamic and seismic stresses.

### INTRODUCTION

Loads induced by ground shaking are different in, above and below the ground structures. While surface structures are loaded mainly by inertial forces in relation to structural masses, the underground structures, due to the high grade of constraint, very low inertial forces are experienced. In Table 1 the major conceptual differences in handling the two phenomena are resumed. Seismic loads due to pure soil shaking in underground structures are thus induced by the relative displacements caused in the medium by the seismic wave propagation. The possible loads induced by seismic

waves on tunnels are due to seismic waves propagating in the longitudinal direction of the tunnel (Figure 1a and 1b) and seismic waves hitting the tunnel in the plane of the cross section (Figure 1c). While longitudinal loads are generally not critical for overall stability (mainly radial deformations are induced that can be partly absorbed by radial joints in lining), the ovaling of the cross section that is induced by shear waves propagation is critical and can induce the failure of the lining. The phenomenon can be sketched as in Figure 2.

Damage to underground structures due to earthquakes has been investigated by several researchers including e.g., Wang et al. (2001), among others. The underground structures should be considered vulnerable to the effects of ground shaking, as demonstrated by the recent events, e.g., 1995 Kobe (Japan), 1999 Chi-Chi (Taiwan) and 2004 Niigata (Japan) earthquakes where several tunnels and underground structures have suffered severe damages. Therefore, it is essential for the tunnel design to account for the seismic load effects as well as the dynamic effects of the travelling train loads besides the static load effects. In this research, the effects of dynamic loads and seismic action on GCML3, Phase 1 (extended from Attaba to Abassia) tunnel were studied employing the finite element program PLAXIS®.

**Table 1. Difference in Seismic Analysis for Underground & Surface Structures.**

Seismic Loads to Structures due to Ground Shaking		
	Surface structures	Underground structures
Phenomenon	The soil surface vibrates and the structure oscillates causing inertial forces	The seismic waves propagating in the medium induce drifts in the structure.
Loads	Load introduced by seismic forces (proportional to accelerations)	Load introduced by seismic strains (proportional to velocities)
Interaction	In common problems is possible to neglect soil-structure interaction	Not possible to neglect soil-structure interaction
Analysis	In common problems linear analyses are possible	Highly non-linear approach

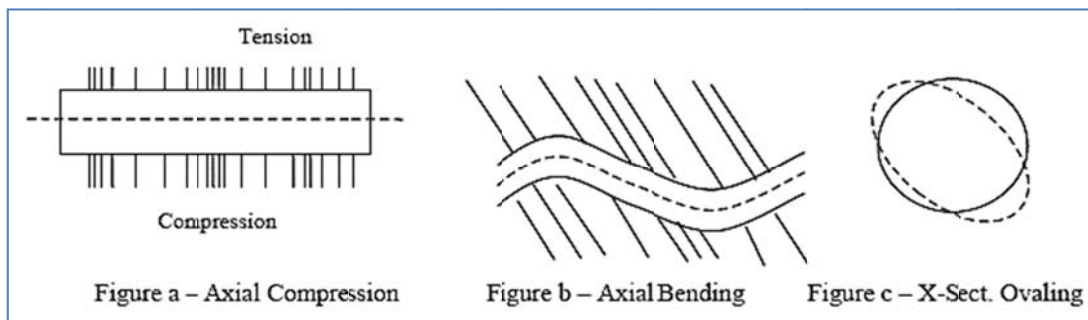


**Figure 1. Seismic load on tunnel lining.**

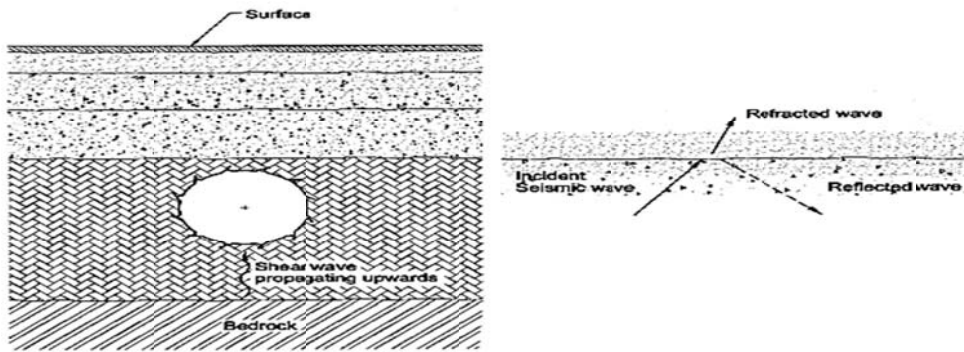


Figure 2. Deformations induced by seismic shear.

**PROJECT DESCRIPTION**

Greater Cairo underground metro is considered as one of the most important national transportation projects. It consists of three lines (Fig. 3) linking the capital major districts with the city center. Greater Cairo Metro Line Three (GCML3) will extend from Imbaba to Cairo Airport and it will be constructed in four phases with total length of about 33 km, (Dawood 2011).

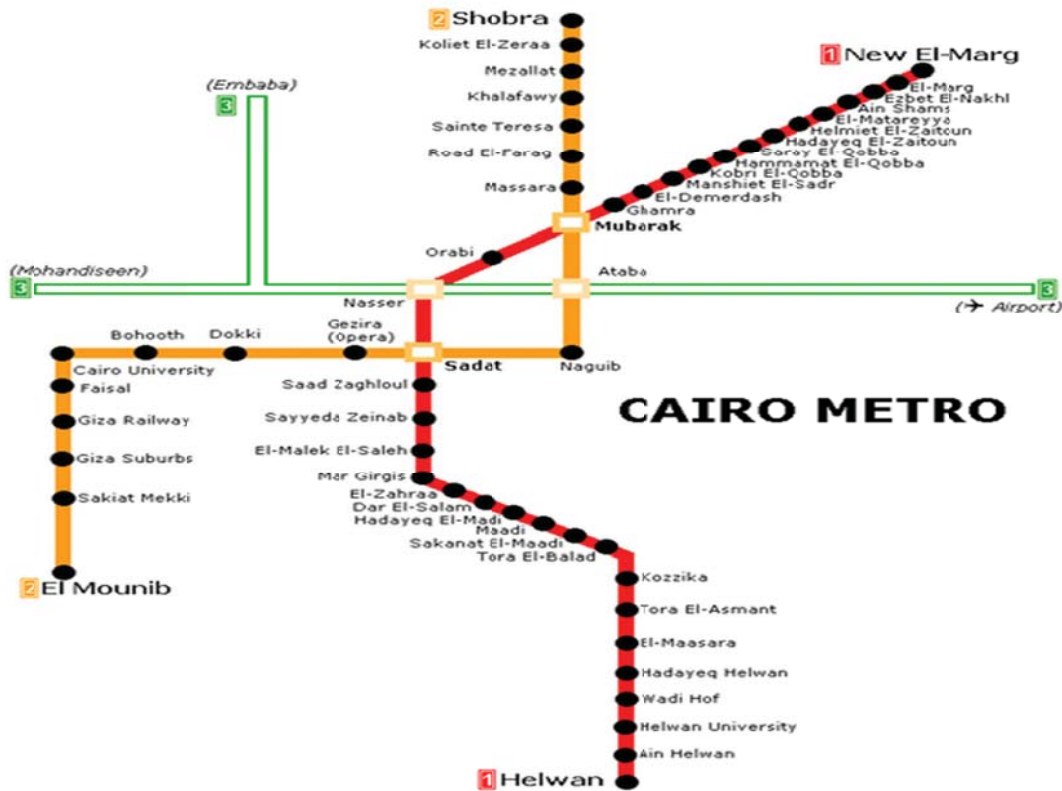


Figure 3. Greater Cairo Metro Lines.

The tunnel has a circular cross section executed by slurry shield Tunnel Boring Machine (TBM) as shown in Figure 4. The tunnel has an internal diameter of 8.35m, external diameter of 9.15m and a precast segmental lining thickness of 0.4m. The elevation of the bottom level of the tunnel is ranging between (+12.30m) and (-17.55m) from mean sea level. The longitudinal alignment has been designed with 2000 meter minimum vertical radius curve. The longitudinal profile is “U” shaped with low point in-between stations so as to guarantee the maximum overburden above the tunnel crown along the route whilst at the same time minimizing stations’ depth. Along the tunnel route, the minimum soil cover over the tunnel crest is not less than 1.2D (1.2 x external tunnel diameter) from ground level.



Figure 4. Greater Cairo metro line 3 tunnel - phase 1.

## SUBSURFACE CONDITIONS

A detailed ground investigation was carried out by the National Authority for Tunnels prior to tunnel construction, employing a wide range of techniques including rotary drilling and sampling for laboratory testing, piezometer tests, and standard penetration tests (NAT, 2007). The soil formations along the tunnel route are typical Cairo Nile Alluvial Deposits. The water table was ranging between 2.5 to 6 m below the ground surface. A representative borehole was used to represent the soil profile. Figure 5 shows the underlying formation at the selected section with the various stratigraphic units. The soil properties considered in the Finite Element Model was based on the soil formation appeared in the representative borehole. Table 2 summarises the properties of each layer where  $\gamma$  stands for the unit weight,  $E$  stands for Young's modulus,  $\nu$  for Poisson's ratio,  $C$  is for cohesion,  $G_{max}$  represents the maximum shear modulus and  $V_s$  denotes the shear wave velocity. These parameters were used as input data to the well-known software EERA<sup>®</sup> to obtain the required damping and dynamic shear modulus parameters to be used in PLAXIS<sup>®</sup>, (Brinkgreve *et. al.*, 2002). More details can be found in Soliman (2013).



Figure 5. Representative Soil Profile in GCML3.

Table 2. Initial Soil Dynamic Parameters Assigned to EERA

Soil Type	$\gamma$ (kN/m <sup>3</sup> )	E(dyna) (MPa)	$\nu$ (dyna)	$\phi$ (dyna) (degree)	C (dyna) (kPa)	Gmax (dyna) (MPa)	Vs (m/sec)
Fill	17	60	0.35	25	0	22.22	113.24
Sand	19.5	245	0.35	36	0	90.741	213.66
Gravel and Sand	20	640	0.35	38	0	237	341
Sand	19.5	540	0.35	36	0	200	317.2

### DYNAMIC LOADS

Two types of dynamic loads were used in the analysis of the tunnel section. Seismic load and train induced dynamic load. In the numerical computation, the earthquake loading is often imposed as an acceleration time-history at the base of the model. To highlight the influence of the input motion on the nonlinear seismic response of a soil layer, three earthquake signals were considered to represent different levels of seismic events (PEER 2012).

The first is the record of Loma Prieta earthquake. The input motion is specified as an outcrop motion from the acceleration time history recorded at Diamond Heights (EW component) during the 1989 Loma Prieta earthquake which occurred on October 17, 1989. Its epicenter was 65 miles south of San Francisco where most damages occurred. It had a moment magnitude of 6.9 and a surface wave magnitude of 7.1. The duration was 15 to 20 seconds; the ground motion is normalized to a target peak acceleration of 0.1g as given in figure 6 to stand for a weak event.

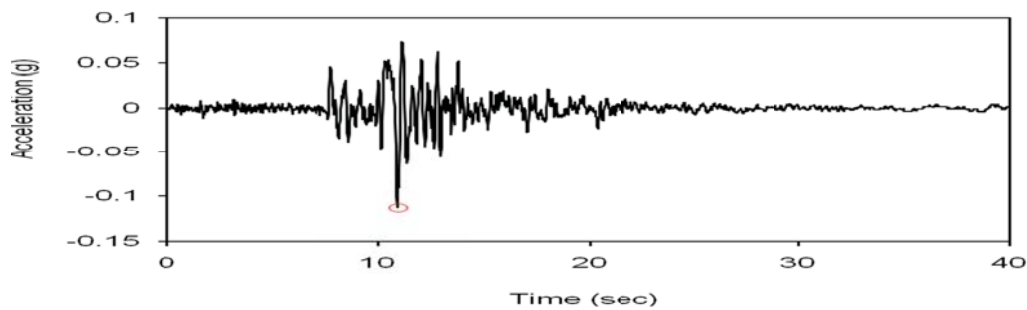


**Figure 6 Time history of acceleration of Loma Prieta earthquake (1989).**

The second is the 1979 Imperial Valley earthquake which occurred at 16:16 Pacific Standard Time on October 15 and impacted southeastern and southern California with the epicenter just south of the international border of the United States and Mexico. It had a magnitude of 6.4 on the moment magnitude scale and a maximum perceived intensity of IX (Violent) on the MM scale. The duration was 20 to 25 seconds; the ground motion is normalized to a target peak acceleration of 0.3g to represent moderate event as plotted in Figure 7.

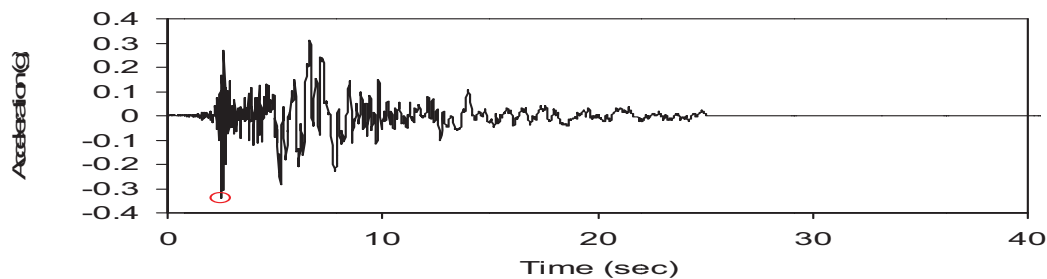


**Figure 7. Time history of acceleration of Imperial Valley earthquake (1979).**

The third is the Northridge earthquake. It occurred at 4:30 a.m. local time on January 17, 1994. Northridge is located about 30 km northwest of Los Angeles. This earthquake had a 6.9 moment magnitude. The hypo-central depth was 19 km. The duration was about 10 seconds to 20 seconds. The earthquake occurred along a "blind" thrust fault close to the San Andreas Fault. The Northridge earthquake was the worst earthquake in the Los Angeles basin since the San Fernando earthquake in 1971, which had a 6.7 magnitude. The ground motion is normalized to a target peak acceleration of 0.45g to stand for the condition of strong event Time history of the normalized Northridge record is plotted in Figure 8.

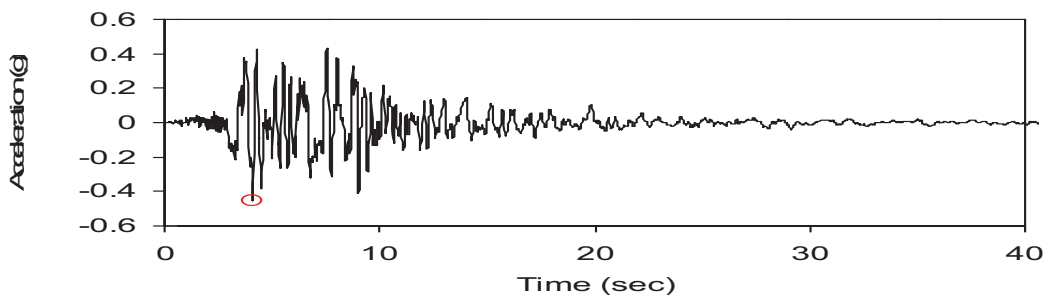


Figure 8. Time history of acceleration of Northridge (1994).

The train induced dynamic load is represented by two concentrated line loads simultaneously applied on the bottom surface of the tunnel lining (Adam *et. al.*, 2001, Adam and Estorff, 2005). The horizontal distance between the two loads is 1.80 m positioned at equal distance on both sides of tunnel centerline. the time history of each load consists of four consecutive impulses; each impulse has a time period of 0.02 seconds and 1 MN in amplitude. Time history for such a load and frequency content for an impulse are given in Figures 9 and 10, respectively. The separation time between each two consecutive impulses is 0.02 seconds. Consequently, the total time period of the applied load is 0.14 seconds. The duration of the unit amplitude of 0.02 s is chosen in such a way that the frequency content of the load covers the typical range of frequencies of vibration as they are caused by heavy axle trains.

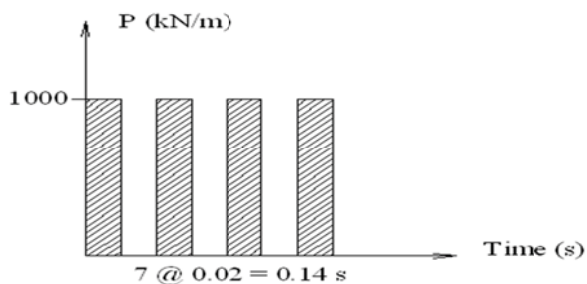


Figure 9. Time history of simulated-train dynamic load.

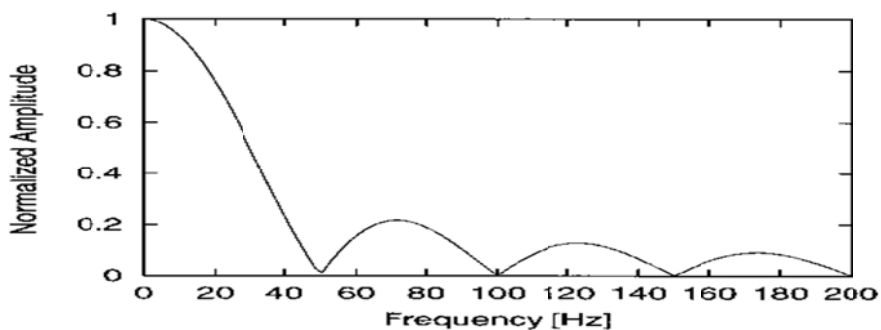


Figure 10. Frequency content of the simulated-train dynamic load.

## NUMERICAL SIMULATION

A realistic simulation of the TBM tunneling dictates considering many factors. A 2D axisymmetric model are not appropriate for urban tunnels as they assume symmetrical field stresses about the tunnel axis, thus neglecting the important effects of ground surface loads. In the analysis of the shallow section under earthquake loads, a 2D plane strain elasto-plastic soil model based on Mohr-Coulomb failure criterion has been developed as shown in Figure 11. In addition to the soil properties given in Table 2, the soil parameters obtained from **EERA**<sup>®</sup> to be assigned to **PLAXIS**<sup>®</sup> model are represented in Tables 3 to 5. The damping ration is given by **D%**, **G(dyna)** determines the dynamic shear modulus,  **$\alpha_R$**  and  **$\beta_R$**  are the Rayleigh damping constants.

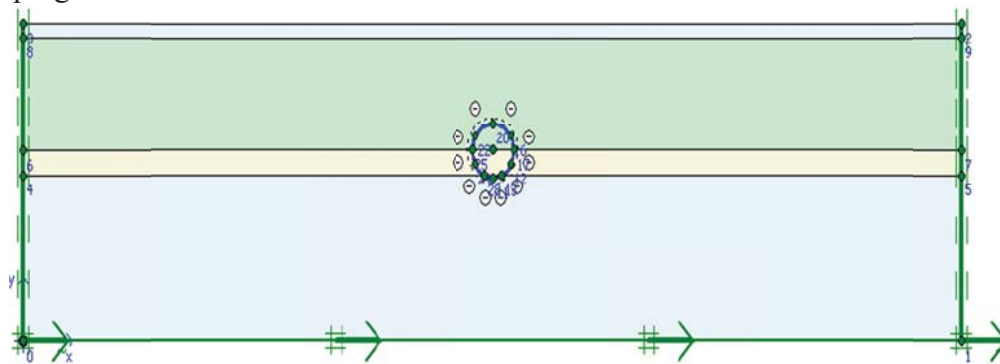


Figure 11. **PLAXIS**<sup>®</sup> 2-plane strain model to study tunnel response under earthquake motion.

In the analysis of the shallow section under train induced dynamic loads, a 2D axisymmetric model with 15-noded elements was used as shown in Figure 12. Single-source vibration problems are often modeled with axisymmetric models. This is because waves in an axisymmetric system radiate in a manner similar to that in a three dimensional system. In this the energy disperses leading to wave attenuations with distance. Geometric damping is generally the most important contribution to the damping of the system.

## EVALUATION OF STRUCTURAL FORCES

The response of Cairo Metro Line 3 tunnel due to seismic excitation using three different amplitudes and durations for the seismic input motion was studied. Earthquakes of Loma Prieta 1989, Imperia Valley 1979 and Northridge 1994 were utilized. Tunnel lining maximum normal forces **N** and maximum bending moments **M** for different seismic motions and train moving load are listed in Table 6 and depicted in Figures 13, 14, 15 and 16.

From the obtained results, it was found that the normal forces on tunnel lining are -828.10 kN/m, -1420 kN/m and -1160 kN/m from Loma Prieta, Imperial Valley and

Northridge earthquakes, respectively. Bending moment values are 62.10 kN.m/m, 549.59 kN.m/m and 495.83 kN.m/m. Straining actions on tunnel lining from train moving load inside the tunnel are 834.51 kN.m/m for normal forces and 179.07 kN.m/m for bending moments which are lower than the results due Imperial valley earthquake and Northridge earthquake. Thus, for low risk earthquake regions, train moving load is critical for design while for moderate or high risk earthquake regions, critical loads will result most probably from the earthquake actions.

The maximum straining actions on tunnel are caused from Imperial Valley earthquake which has 0.30g peak acceleration. The minimum values are caused from Loma Prieta earthquake which has 0.10g peak acceleration. It is very clear that the increase in straining actions values is not in linear relation with the increase of peak acceleration values. This is due to two reasons; first is the different characteristics of earthquake motions which include earthquake peak acceleration and the critical periods where highest energy peaks are concentrated which is known as frequency contents. Secondly, the soil media nonlinear property which means that soil media stiffness and damping ratios are different with nonlinear relation for each earthquake motion depending on the stress-strain hysteresis and energy consumption by the soil media during the ground shaking.

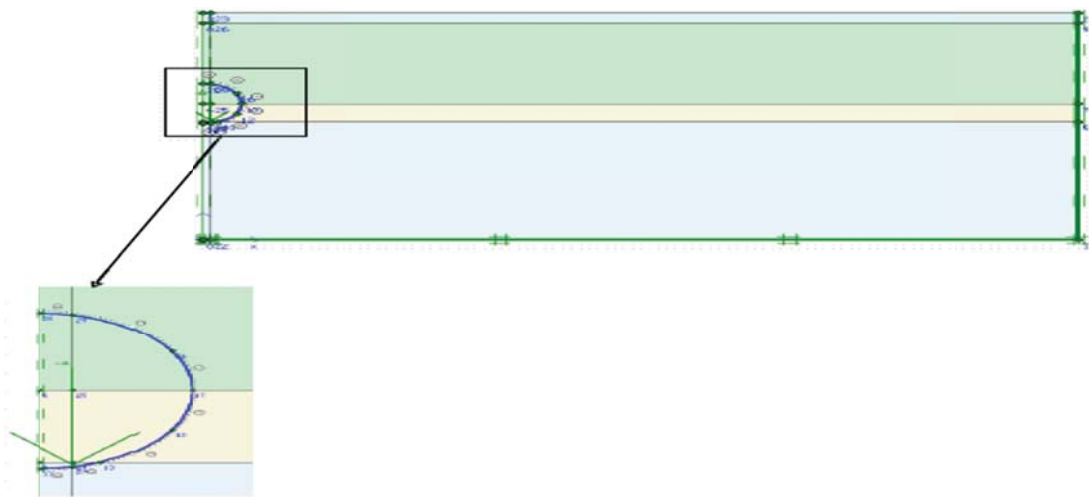


**Figure 12. PLAXIS<sup>®</sup> 2-D axisymmetric model for tunnel response under train moving load.**

Stresses on tunnel lining due to the above mentioned earthquakes and considering uncracked tunnel cross sections, are - 4.40 MPa, 0.258 MPa for compression and tension stresses, respectively, due to Loma Prieta earthquake. For Imperial Valley earthquake, the stresses for tension and compression are -24.16 MPa and 17 MPa, respectively. Finally, for Northridge earthquake, the tension and compression stresses on tunnel lining are -21.50 MPa and 15.6 MPa, respectively. These stresses can be combined with other static stresses to obtain the envelope critical values for the

design. It should be mentioned that the tunnel passes through the city of Cairo which is located at the third seismic zone according the Egyptian Code, ECP201(2012). The expected peak ground acceleration in this zone is 0.15g. Therefore, it can be stated that the concrete cross section of 40 cm can safely sustain the expected values of internal forces due to static, dynamic and earthquake loads.

**Table 3. PLAXIS<sup>®</sup> model soil dynamic parameters for Loma Prieta earthquake**

Soil Type	G(dyna) (MPa)	D%	$\alpha_R$	$\beta_R$
Fill	17.2	3.64	0.47	0.002114
Sand	48.718	7.14	0.922	0.004147
Gravel and Sand	165.94	4.443	0.5737	0.00258
Sand	118.9	5.894	0.761	0.00342

**Table 4. PLAXIS<sup>®</sup> model soil dynamic parameters for Imperial earthquake**

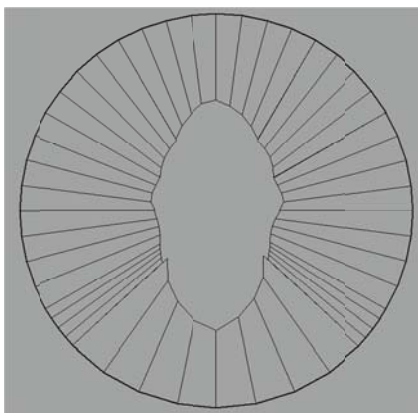
Soil Type	G(dyna) (MPa)	D%	$\alpha_R$	$\beta_R$
Fill	12.156	6.72	0.868	0.00392
Sand	22.478	14.914	1.93	0.00871
Gravel and Sand	95.234	9.248	1.194	0.00533
Sand	43.214	14.6	1.886	0.0086

**Table 5. PLAXIS<sup>®</sup> model soil dynamic parameters for Northridge earthquake.**

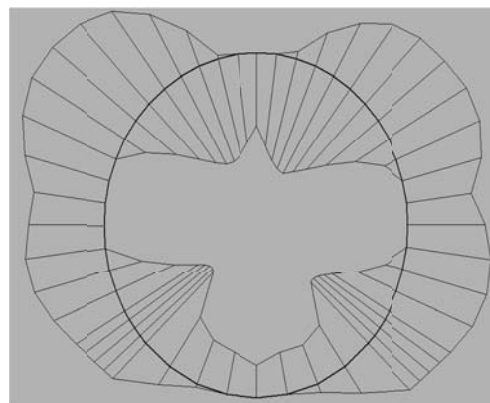
Soil Type	G(dyna) (MPa)	D%	$\alpha_R$	$\beta_R$
Fill	14.8	4.8	0.62	0.0028
Sand	31.925	11.591	1.5	0.00677
Gravel and Sand	117.27	7.63	0.985	0.0044
Sand	59.7633	11.94	1.542	0.007

**Table 6. Tunnel Straining Actions under Loma Prieta, Imperial, Northridge Earthquakes and Train Moving Load**

Loma Prieta		Imperial		Northridge		Train Moving Load	
N env. (kN/m)	M env. (kN.m/m)	N env. (kN/m)	M env. (kN.m/m)	N env. (kN/m)	M env. (kN.m/m)	N env. (kN/m)	M env. (kN.m/m)
-828.10	62.10	-1420	549.59	-1160	495.83	834.51	179.07

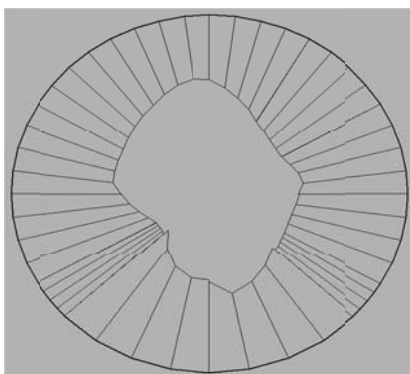


a) Envelope normal force diagram  
N.F.= - 828.10kN /m

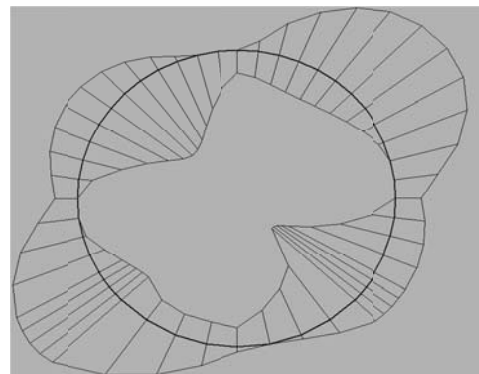


b) Envelope bending moment diagram  
B.M.= 62.10kN.m/m

**Figure 13. Loma Prietaearthquake:(a) Normal forces and (b) Bending moments.**

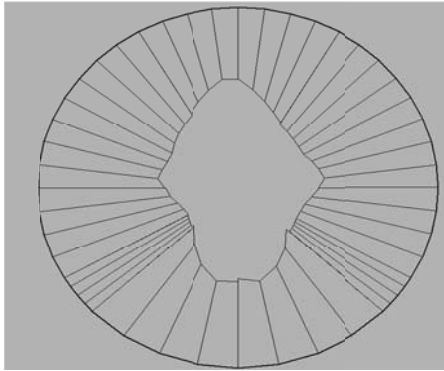


a) Envelope normal force diagram  
N.F.= -1420kN /m

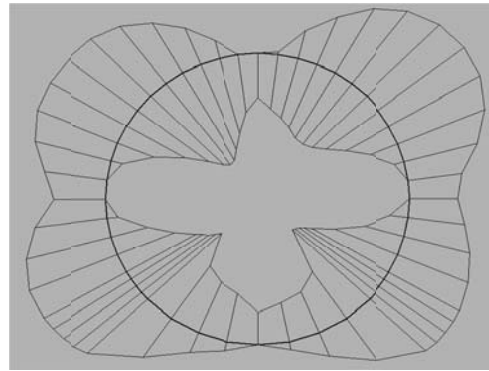


b) Envelope bending moment diagram  
B.M.= 549.59kN.m/m

**Figure 14. Imperial earthquake: (a) Normal forces and (b) Bending moments.**

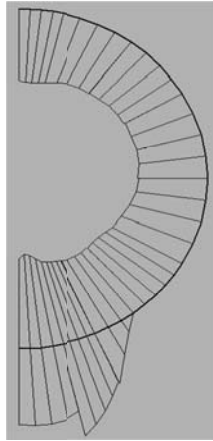


a) Envelope normal force diagram  
N.F.= -1160kN /m

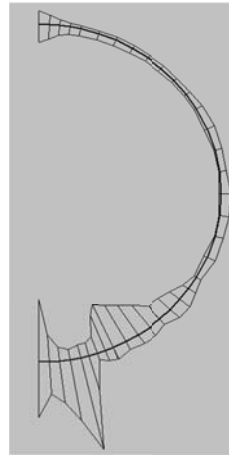


b) Envelope bending moment diagram  
B.M.= 495.83kN.m/m

**Figure 15. Northridge earthquake: (a) Normal forces and (b) Bending moments.**



a) Envelope normal force diagram  
N.F.= 834.51kN /m



b) Envelope bending moment diagram  
B.M.= 179.07kN.m/m

**Figure 16. Train load: (a) Normal forces and (b) Bending moments in tunnel.**

## CONCLUSIONS

The following points are the main conclusions of this research:

- Greater Cairo metro line 3 of concrete cross section of 40 cm can safely sustain the moderate values of internal forces due to the expected earthquake loading.
- For low risk earthquake regions, train moving load is critical while for moderate or high risk earthquake regions, critical loads are from earthquake motions.

- Use of a hysteretic damping model to represent the soil/rock degradation during seismic ground motions is reasonable for the dynamic analysis of the Cairo Tunnel, and can appropriately capture the anticipated ground response.
- Dynamic analysis can produce more realistic results since it can account for various load combinations considered in the tunnel design.

## REFERENCES

- Adam, M., Pflanz, G. and Schmid, G. (2000). "Two- and three-dimensional modelling of half-space and train track embankment under dynamic loading." *Soil dynamics and Earthquake Engineering*, Elsevier Science, UK, 19(8), 559-573.
- Adam, M., and von Estorff, O. (2005) "Reduction of train-induced building vibrations by using open and filled trenches." *Computers and Structures*, 83(1), 11–24.
- Dawood, W., A. (2011), "Finite difference modeling for determination of tunneling effects on adjacent structures." *M.Sc. Thesis*, Department of Civil Engineering, Faculty of Engineering-Shobra, Benha University, Egypt.
- ECP-201 (2012). "Egyptian code for calculating loads and forces in structural work and masonry." *Housing and Building National Research Center*, Ministry of Housing, Utilities and Urban Planning, Cairo, Egypt
- NAT (2007). National Authority for Tunnels Report No. Annex (8A), Contract No. 49 /Metro, "Geotechnical Investigation Report for Egyptian – French JV for Civil Works, Greater Cairo Metro Line No. 3, Cairo Airport to Imbaba Stations. Phase 1 from Attaba to Abbasia Stations." Cairo, Egypt.
- PEER (2012). "PEER strong motion database." <http://peer.berkeley.edu/smcat/search.html>. Accessed 10 Jul 2010.
- Brinkgreve RBJ, Al-Khoury R, Bakker KJ, Bonnier PG, Brand PJW, Broere W, et al. (2002) "Plaxis finite element code for soil and rock analyses." The Netherlands: Balkema Publisher.
- Soliman, M. F. (2013). "Study of tunnel response to dynamic loadings), *M. Sc. Thesis*, Department of Civil Engineering, Faculty of Engineering-Shobra, Benha University, Egypt.
- Wang, W. (2001). "Assessment of damage in mountain tunnels due to the Taiwan Chi-Chi Earthquake." *J. Tunneling and Underground Space Technology*, 16, 133–150.